

Ferrimagnetic organelles in multicellular organisms

Gorobets S. V.¹, Gorobets O. Yu.^{1,2}, Gorobets Yu. I.^{2,1}, Bulaievska M. O.¹

¹National Technical University of Ukraine "Igor Sikorsky Kyiv Polytechnic Institute", 03056, Kyiv, Ukraine

²Institute of Magnetism NAS of Ukraine and MESYS of Ukraine, 03142, Kyiv, Ukraine

Abstract

Introduction

Biogenic ferrimagnetism has been intensively studied for more than four decades in connection with the discovery of biogenic magnetic nanoparticles (BMN) in a wide variety of organisms¹⁻⁴⁰. In the narrow sense, BMNs are nanoparticles of strong natural magnets (ferrites – magnetite, maghemite, greigit) in organisms that create stray magnetic fields in their vicinity^{41,42}. In a broad sense, BMNs are nanoparticles of iron-containing materials that have sufficient magnetic susceptibility for movement in the magnetic field of laboratory magnets¹⁰. These nanoparticles are called biogenic because their biosynthesis is programmed at the genetic level⁴¹⁻⁴³. The main impetus for the study of biogenic ferrimagnetism was the ability of magnetotactic bacteria to move along the lines of force of the Earth's magnetic field (i.e. magnetotaxis)^{1,2}. Subsequently, the idea of magnetotaxis was developed into the idea of magnetoreception of animals (i.e. their ability to orient in the geomagnetic field) due to the presence of BMN^{9,33}.

But when examining organs and tissues for the presence of BMN, these magnetic nanoparticles were found not only in those organs and tissues that may be responsible for the orientation of animals in the Earth's external magnetic field (brain, beak of migratory birds, lateral line and ethmoid bone of migratory fish), but also in a number of other organs, both migratory and non-migratory organisms^{8,14,19,22,24,25,28-30,33,37-39,44-50} (Fig. 1, Table 1).

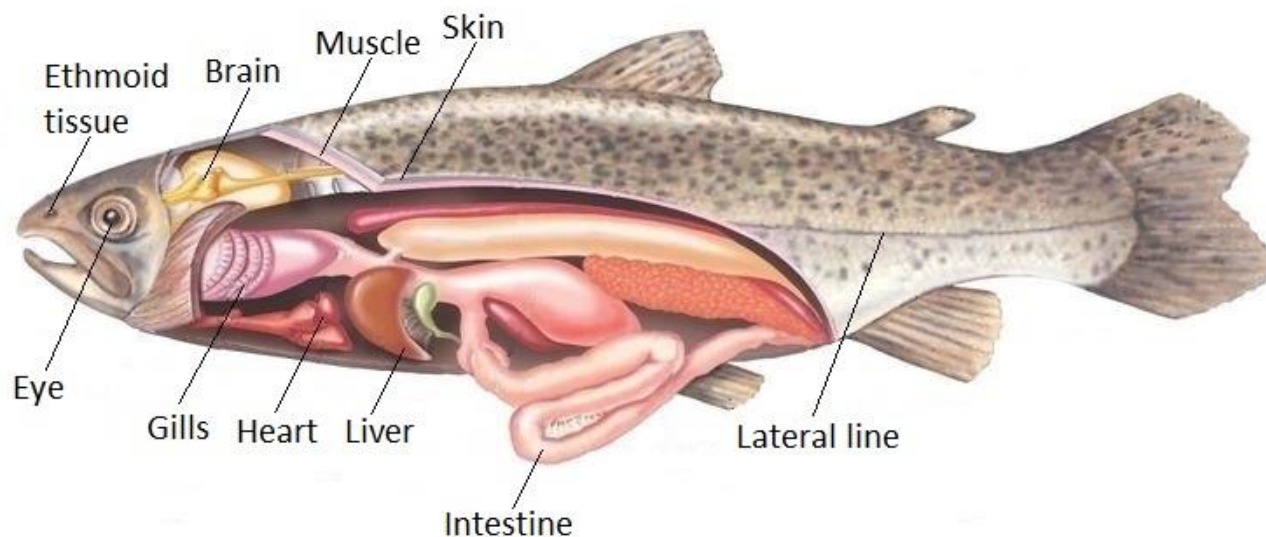


Fig. 1. The organs of migratory fish, in which the presence of BMNs is experimentally shown: ethmoid bone^{22,45,46,51}, brain^{19,22,45}, muscle^{22,45,46}, skin^{22,45,46,51}, eye^{22,45,46,51}, gills⁴⁵, heart⁴⁵, liver⁴⁵, intestine⁴⁵, lateral line^{22,45}. The organs of non-migratory fish, in which the presence of BMNs is experimentally shown: ethmoid bone, brain, lateral line^{24,25}.

All these numerous experimental data on the detection of BMNs in analogous and homologous organs of organisms of different phylogenetic groups confirm the existence of the theoretically predicted single genetically programmed mechanism of biosynthesis of BMNs in all organisms^{42,52,53}. At the same time, the theoretically predicted presence of BMNs in a number of human organs and tissues by the methods of comparative genomics⁵⁰ is confirmed by experimental studies on the presence of BMNs in human organs^{34,37,38,54-56}, as well as analogous and homologous organs and tissues of animals^{8,14,19,22,25,33,44-47,49,50} (Table 1).

Table 1. Human organs, as well as analogous and homologous organs of animals, in which BMNs are found.

Human organs with theoretically predicted BMNs presence (+)	Experimentally confirmed BMNs presence in human organs	Experimentally confirmed BMNs presence in relevant or analogous fish organs
Brain ⁵⁰ (+)	Brain ^{34,54,55}	Brain of the <i>Oncorhynchus nerka</i> ¹⁹ , brain of the whale <i>Megaptera novaeangliae</i> ⁴⁴ , head <i>Pachycondyla marginata</i> ¹⁴ , brain of the silver carp (Fig. 9)
Heart ⁵⁰ (+)	Heart ³⁷	Heart of the <i>Sus domestica</i> ⁴⁹ , fish heart ⁴⁵
Liver ⁵⁰ (+)	Liver ³⁷	Liver of the <i>Sus domestica</i> ⁴⁹ , fish liver ⁴⁵ , liver of the house mouse <i>Mus musculus</i> (Fig. 2, 3)
Spleen ⁵⁰ (+)	Spleen ³⁷	Spleen of the <i>Sus domestica</i> ⁵⁰
Ethmoid bone ⁵⁰ (+)	Ethmoid bone ⁵⁶	Ethmoid bone of the <i>Salmo salar</i> , ethmoid bone of the <i>Cyprinus carpio</i> , ethmoid bone of the <i>Esox lucius</i> ²⁵ , ethmoid bone of the <i>Oncorhynchus nerka</i> ⁸ , ethmoid bone of the <i>Delphinus delphis</i> ³³ , ethmoid bone of the <i>Thunnus albacares</i> ⁴⁶ , antennas of the <i>Pachycondyla marginata</i> ¹⁴
Adrenal glands ⁵⁰ (+)	Adrenal glands ³⁸	
Lung ⁵⁰ (+)		Lung of the <i>Sus domestica</i> ⁴⁹ , fish gills ⁴⁵
Kidney ⁵⁰ (+)		Kidney of the <i>Sus domestica</i> ⁵⁰
Intestine ⁵⁰ (+)		Intestine of the fish ⁴⁵ , abdominal cavity of the ants ¹⁴ , intestine of the house mouse <i>Mus musculus</i> (Fig. 5)
Muscle tissue ⁵⁰ (+)		Muscle of the fish ^{22,46}
Skin ⁵⁰ (+)		Skin of the <i>Salmo salar</i> ²² , skin of the <i>Oncorhynchus nerka</i> ⁴⁷ , skin of the <i>Thunnus albacares</i> ⁴⁶
Eyes		Eyes of the fish ^{22,45}
Joints		Joints of the <i>Pachycondyla marginata</i> ¹⁴

In this work, the localization of BMNs was investigated using atomic force (AFM) and magnetic force microscopy (MFM) in a number of organs of various organisms (animals, plants, fungi) in order to identify which systems of multicellular organisms include BMNs.

Experiment and discussion

In this paper, the following samples were examined using AFM and MFM, namely, animal samples: liver, intestine, pancreas of mouse, lungs, kidneys, spleen of pig, brain of carp; plant samples: leaves and root of tobacco, stem and tuber of potato; and fungi samples: fruit bodies of the common and shiitake mushrooms. The cells and other structural components (shown in the images by arrows) in the samples of the listed organs were identified and the localization of BMNs in the indicated organs was shown.

The results of studies of samples of the liver of a mouse with the use of AFM and MFM showed that BMNs in the liver of a mouse are located in the wall of sinusoids (capillaries of the liver) (Fig. 2-3 and Table 2). Sinusoids⁵⁷, sinusoidal endothelial cells of the liver⁵⁸, nuclei of sinusoidal endothelial cells of the liver^{57,59}, hepatocytes, nuclei of hepatocytes⁵⁷, fenestrae⁵⁸⁻⁶¹ presented in Fig. 2-3 in this paper have typical morphology and dimensions, characterized in the works⁵⁷⁻⁶¹.

Table 2. Dimensional characteristics of the structural components of the mouse liver

Structural components	Calculated dimensions (see Fig. 2-3), μm	Dimensions in literature, μm	References
Capillary density	400-600/ μm^2	400-500/ μm^2	62
Sinusoids	5-20	5-15	63-65
Sinusoidal endothelial cells	15-25	20-25	58
Hepatocytes	15-25	20-30	58
Hepatocyte nuclei	5-8	6-8	58
Fenestrae	200-500	50-500	58-61

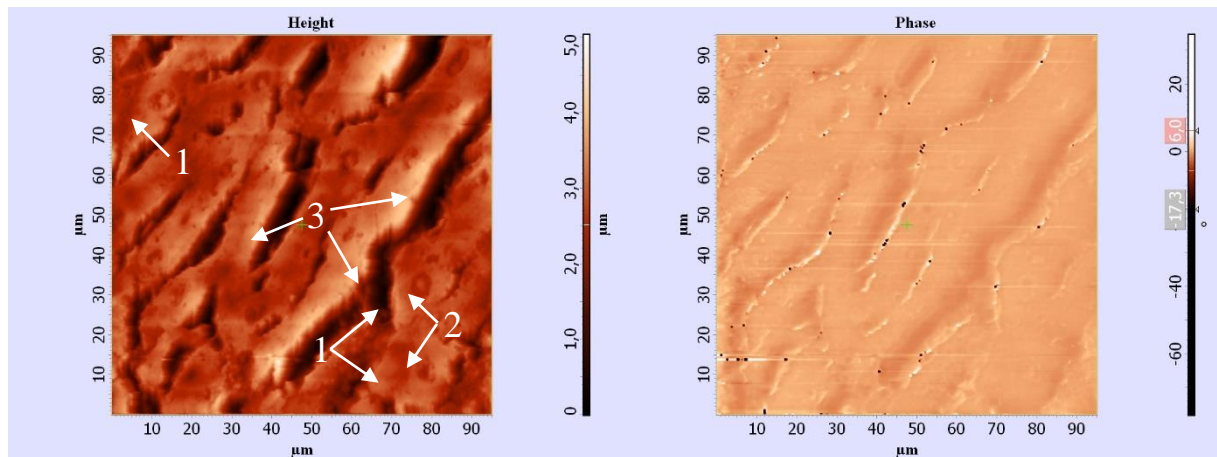


Fig. 2. AFM (left) and MFM (right) images of a sample of the liver of the house mouse *Mus musculus*: 1 hepatocyte, 2 nuclei of hepatocytes and 3 sinusoids.

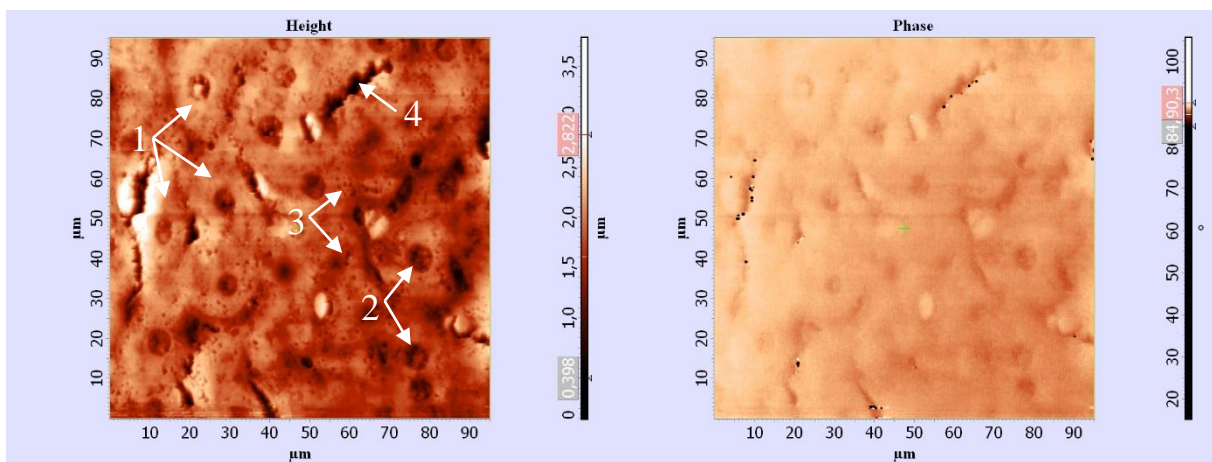


Fig. 3. AFM (left) and MFM (right) images of a sample of the liver of the house mouse *Mus musculus*: 1 sinusoidal endothelial cells of the liver, 2 nuclei of sinusoidal endothelial cells of the liver, 3 fenestrae and 4 sinusoids.

Similar results were obtained on the localization of BMNs in the samples of the pancreas and intestines of a mouse. So, BMNs in the pancreas and the intestines of the mouse are located in the wall of the capillaries as can be seen from Figures 4-5 and data on the size and distance between the capillaries in Tables 3-4. The capillaries of the pancreas are shown in Fig. 4 in this paper and have typical morphology and size⁶⁶⁻⁶⁸.

Table 3. Dimensional characteristics of the structural components of the mouse pancreas

Structural components	Calculated dimensions (see Fig. 4), μm	Dimensions in literature, μm	References
Distance between the capillaries	10-30	20-50	66
Capillaries	4-10	3-7	66-68

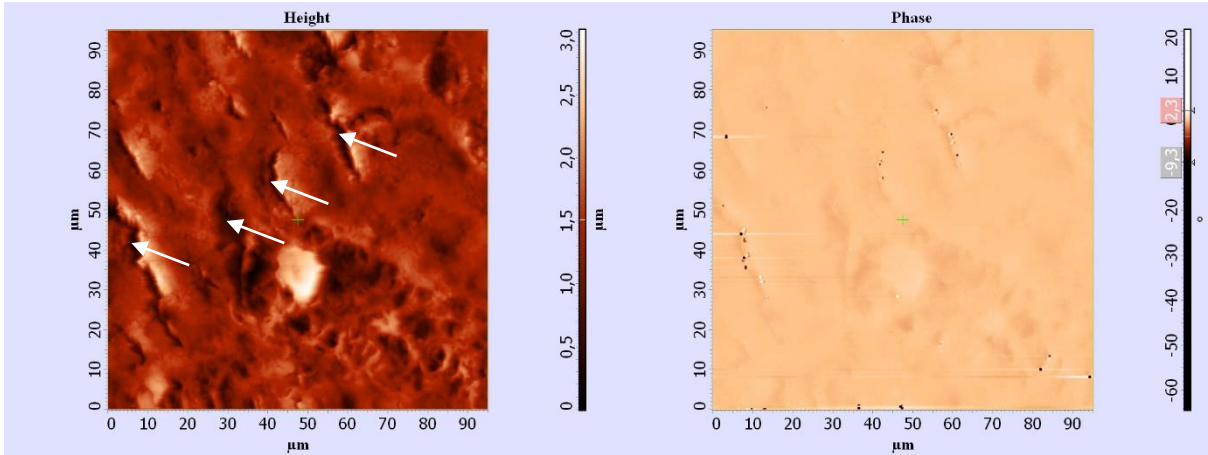


Fig. 4. AFM (left) and MFM (right) images of a sample of the pancreas of the house mouse *Mus musculus*: arrows indicate the capillaries.

Capillaries of the intestine are presented in Fig. 5 in this work and have also typical morphology and size, described in the work^{69,70}.

Table 4. Dimensional characteristics of the structural components of the mouse intestine

Structural components	Calculated dimensions (see Fig. 5), μm	Dimensions in literature, μm	References
Distance between the capillaries	5-30	30-40	71,72
Capillaries	3-6	3-5	69,70

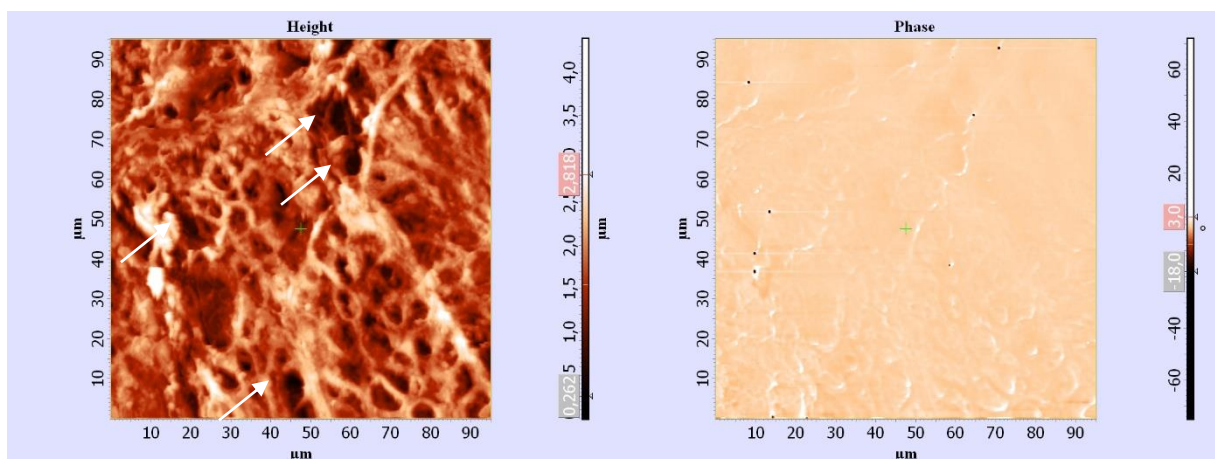


Fig. 5. AFM (left) and MFM (right) images of a sample of the intestine of the house mouse *Mus musculus*: arrows indicate the capillaries.

AFM and MFM examinations of porcine specimens gave similar results, namely, BMNs in the lungs (Fig. 5 and Table 6), kidneys (Fig. 6 and Table 7) and spleen (Fig. 7 and Table 8) of the pig are located in the capillary wall. So, capillaries of lungs, are presented in fig. 6 in this paper and have typical morphology and size, described in the works^{73,74}.

Table 5. Dimensional characteristics of the structural components of the pig lung

Structural components	Calculated dimensions (see Fig. 6), μm	Dimensions in literature, μm	References
Distance between the capillaries	5-25	10-20	73
Capillary density	600-900/ μm^2	700-900/ μm^2	75-78
Capillaries	5-10	5-20	73,75

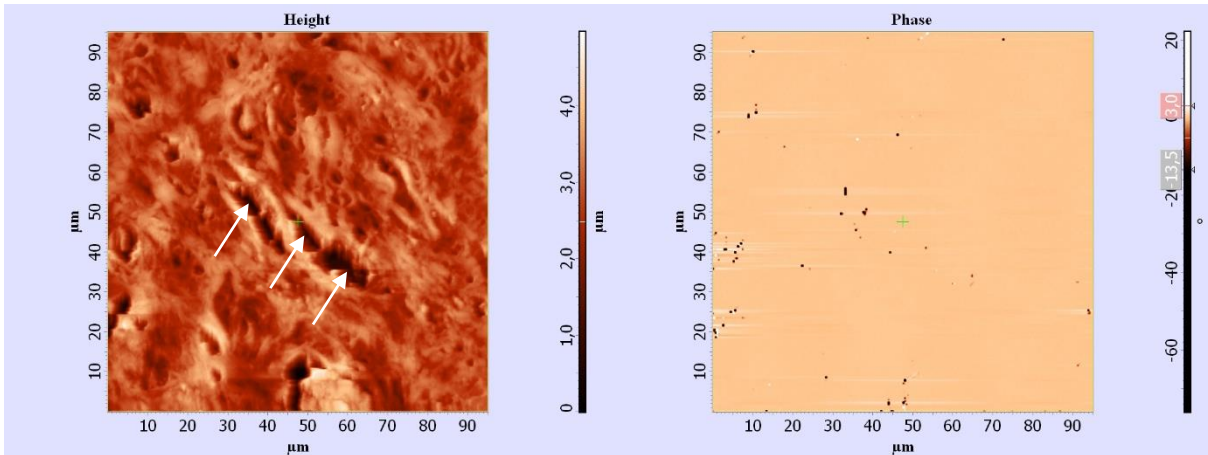


Fig. 6. AFM (left) and MFM (right) images of a sample of the lungs of a domestic pig *Sus domestica*: arrows indicate the capillaries.

The capillaries of the kidneys are presented in Fig. 7 in this paper and have typical morphology and size, described in⁷⁹.

Table 6. Dimensional characteristics of the structural components of the pig kidney

Structural components	Calculated dimensions (see Fig. 7), μm	Dimensions in literature, μm	References
Capillary density	100-300/ μm^2	25-220/ mm^2	80,81
Capillaries	7-10	3-20	82,83

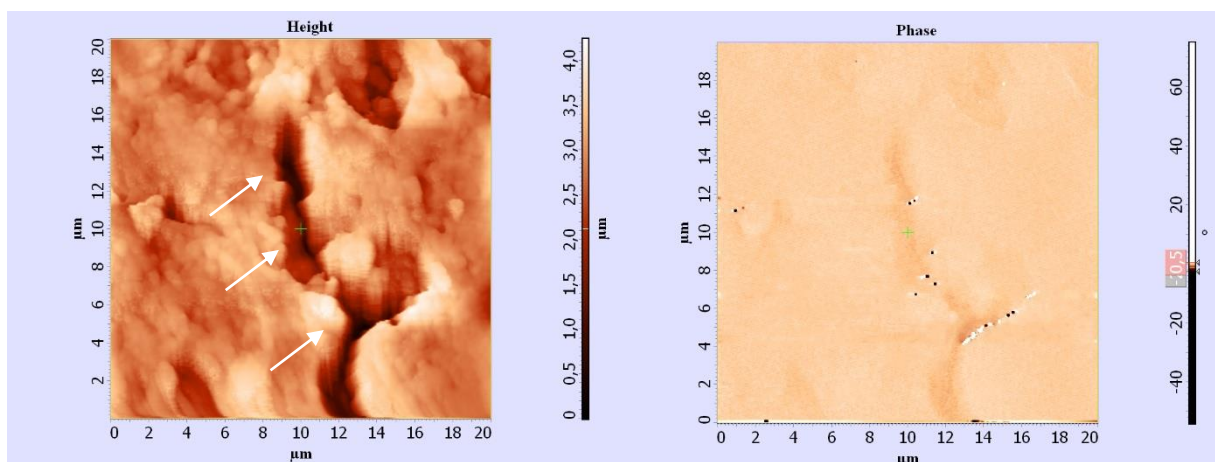


Fig. 7. AFM (left) and MFM (right) images of a sample of the kidney of the domestic pig *Sus domestica*: arrows indicate the capillaries.

The capillaries of a spleen, are presented in fig. 8 in this work, have typical morphology and size, described in^{84,85}.

Table 7. Dimensional characteristics of the structural components of the pig spleen

Structural components	Calculated dimensions (see Fig. 8), μm	Dimensions in literature, μm	References
Distance between the capillaries	5-10	10-30	86
Capillaries	4-7	4-10	87-90

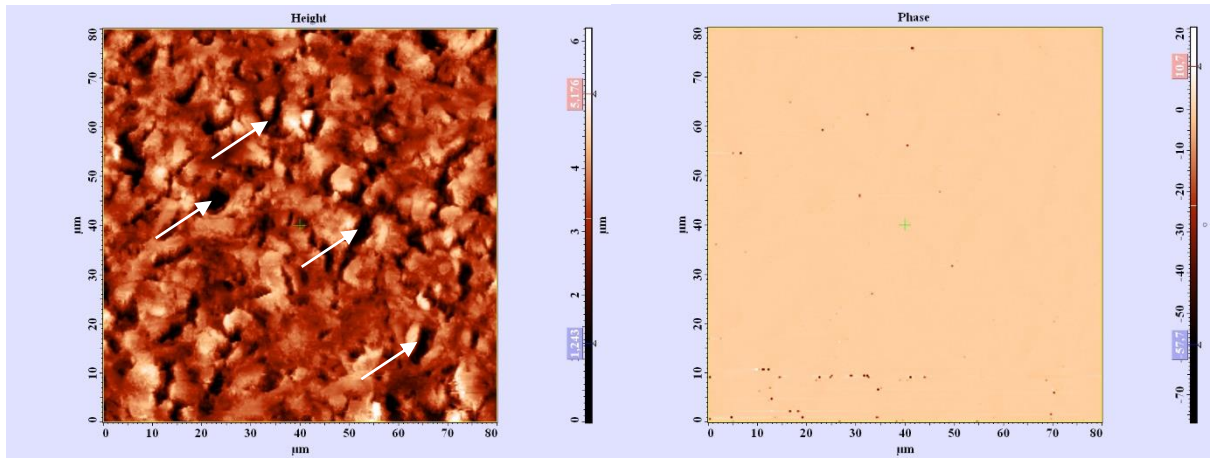


Fig. 8. AFM (left) and MFM (right) images of a sample of the spleen of the domestic pig *Sus domestica*: arrows indicate the capillaries.

As noted above, BMNs are most thoroughly investigated in the organs and tissues of fishes. However, only transmission electron microscopy (TEM) and MFM provide information on the location of BMNs among all experimental methods that are used today to study BMNs^{34,35,91-114}. This paper presents the results of AFM and MFM studies of samples of the silver carp brain, and it is shown that BMNs are located in the capillary wall (Fig. 9 and Table 8) in the brain of the silver carp, as in the organs of mice and pigs. The capillaries of brain are presented in fig. 9 in this work and have typical morphology and dimensions, characterized in¹¹⁵.

Table 8. Dimensional characteristics of the structural components of the silver carp brain

Structural components	Calculated dimensions (see Fig. 9), μm	Dimensions in literature, μm	References
Distance between the capillaries	10-30	15,3	116
Capillaries	3-9	3-8	116,117

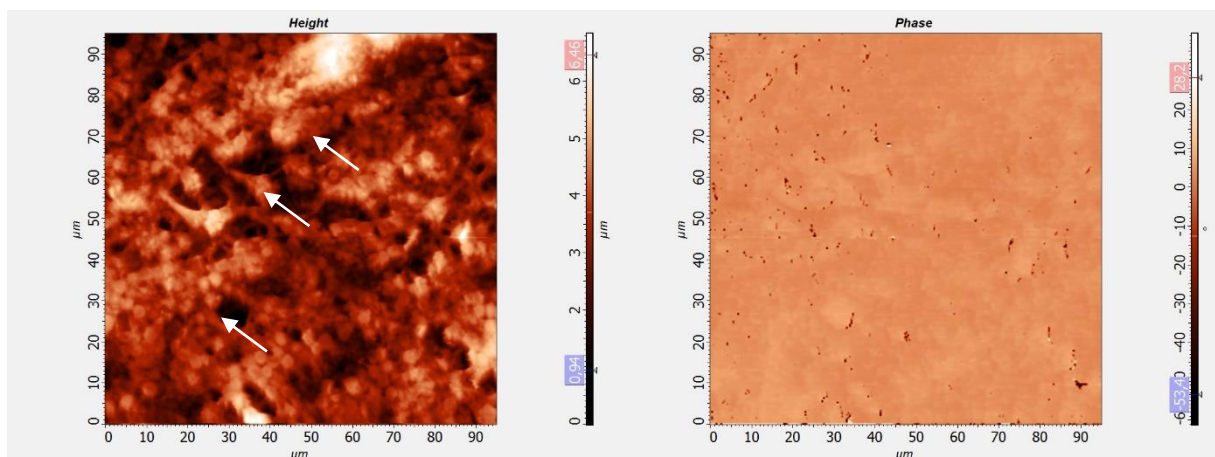


Fig. 9. AFM (left) and MFM (right) images of a sample of the silver carp brain of *Cyprinus carpio*: arrows indicate the capillaries.

The BMNs in the human ethmoid bone are located in the sinuses of the bone⁵⁶, through which the capillaries and nerves pass¹¹⁸⁻¹²⁰. The location of BMNs in the ethmoid bone of fishes is similar²⁵. Thus, a common feature of the location of BMNs in the ethmoid bone and in other organs of various animals (Fig. 2-9, Table 1) is their localization in the vicinity of the capillaries.

Due to the fact that for many years, BMNs was investigated mainly in connection with the ideas about magnetotaxis and magnetoreception, BMNs in plants and fungi has been little studied. For example, the paper¹¹ presents experimental data on the detection of magnetically sensitive nanoparticles in plants, but the authors of this work consider it more likely that they have detected phytoferritin and its aggregates, and not plant BMNs. As for fungi, BMNs is experimentally detected only in the microfungi *Fusarium oxysporum* and *Verticillium spp.*¹²¹.

The study of BMNs in plants was carried out on the example of tobacco, as the most studied model organism among plants, as well as potatoes. The BMNs in the leaf and the roots of tobacco (Fig. 10-11) are located on the membrane of phloem sieve tubes. Phloem is a conducting plant tissue that forms a network of sieve tubes through which organic substances, synthesized by leaves during photosynthesis, are transported to all plant organs¹²²⁻¹²⁶, unlike xylem, which transports water and minerals from the soil¹²⁷⁻¹³⁰. Sieve tubes of tobacco leaf are presented in Fig. 10 in this paper and have the typical morphology and dimensions described in¹³¹.

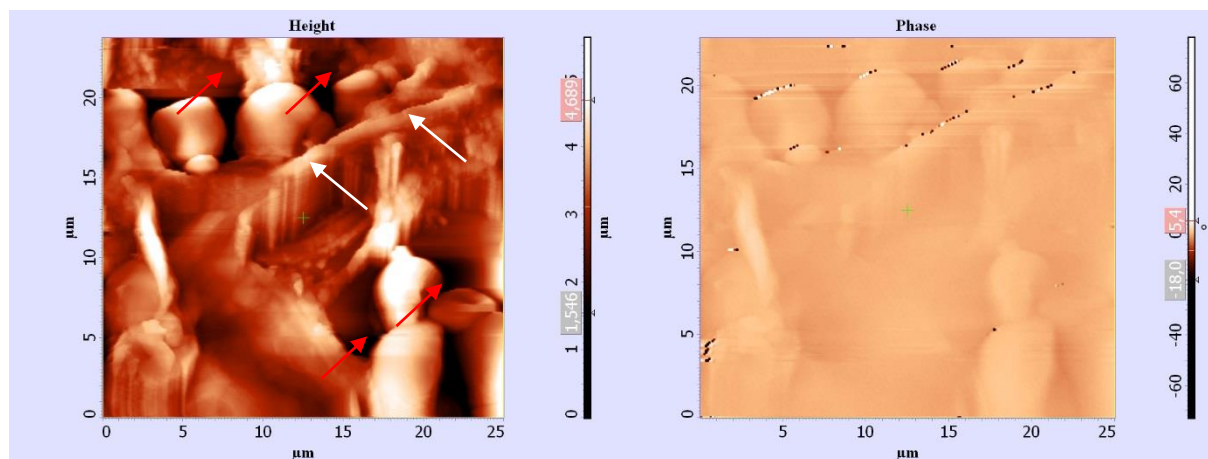


Fig. 10. AFM (left) and MFM (right) images of a sample of a leaf of the cultivated tobacco *Nicotiana tabacum*. Elements of sieve tubes, including pores, are visible in the AFM image. White arrows in the AFM image indicate the membrane of the sieve tubes, red arrows indicate the pores of the sieve tubes.

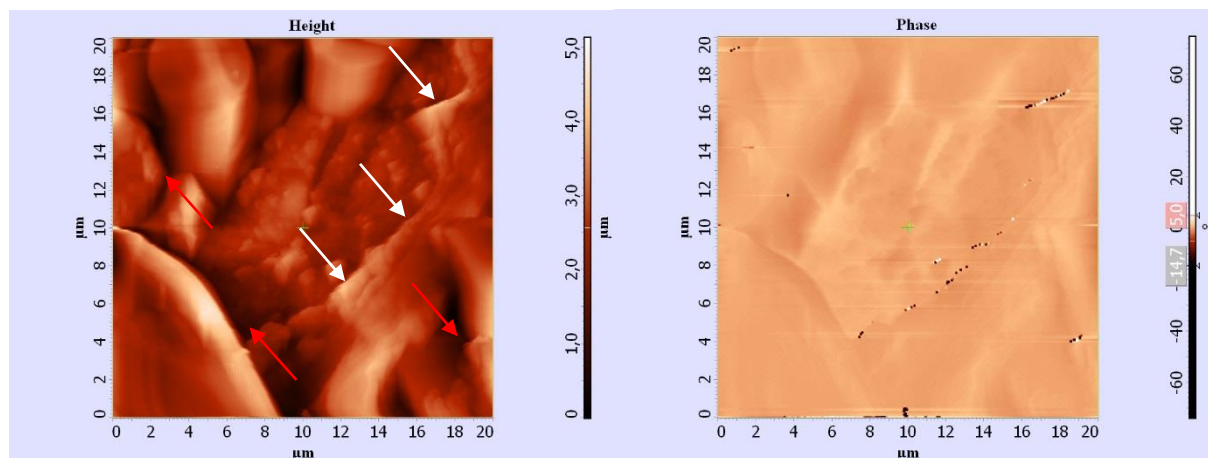


Fig. 11. AFM (left) and MFM (right) images of a sample of a root of the cultivated tobacco *Nicotiana tabacum*. Elements of sieve tubes, including pores, are visible in the AFM image. White arrows in the AFM image indicate the membrane of the sieve tubes, red arrows indicate the pores of the sieve tubes.

Similar data on the location of BMNs were obtained on the samples of potatoes. The BMNs in the potato stalk are located in the walls of the conducting tissue (phloem) (as can be seen from Fig. 12-

13), which is characterized in¹³². BMNs in a potato tuber are located at the boundary between starch grains¹³³ and conducting tissue (phloem).

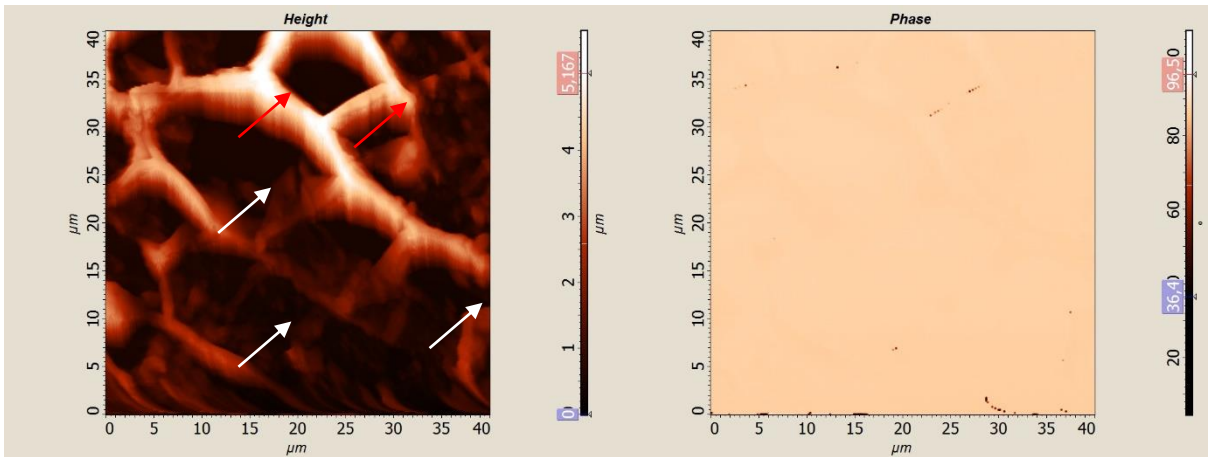


Fig. 12. AFM (left) and MFM (right) images of a sample of the stem of a potato *Solanum tuberosum*: conducting tissue/sieve tubes (white arrows) phloem, cell wall (red arrows).

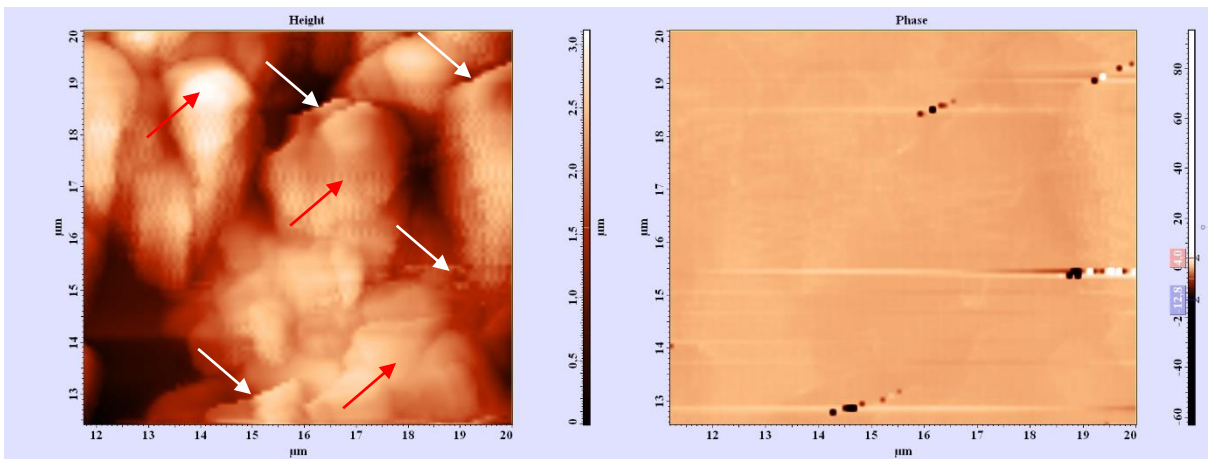


Fig. 13. AFM (left) and MFM (right) images of a sample of the tuber of a potato *Solanum tuberosum*: conducting tissue/sieve tubes (white arrows) phloem, cell wall (red arrows).

The study of BMNs in mushrooms was carried out using the example of higher mushrooms, such as mushrooms *Agaricus bisporus* and *Lentinula edodes*, which are the most common edible mushrooms. As can be seen from Fig. 14-15 BMNs in the mushroom are located in the walls of the vascular hyphae, which are characterized in the works¹³⁴⁻¹³⁶.

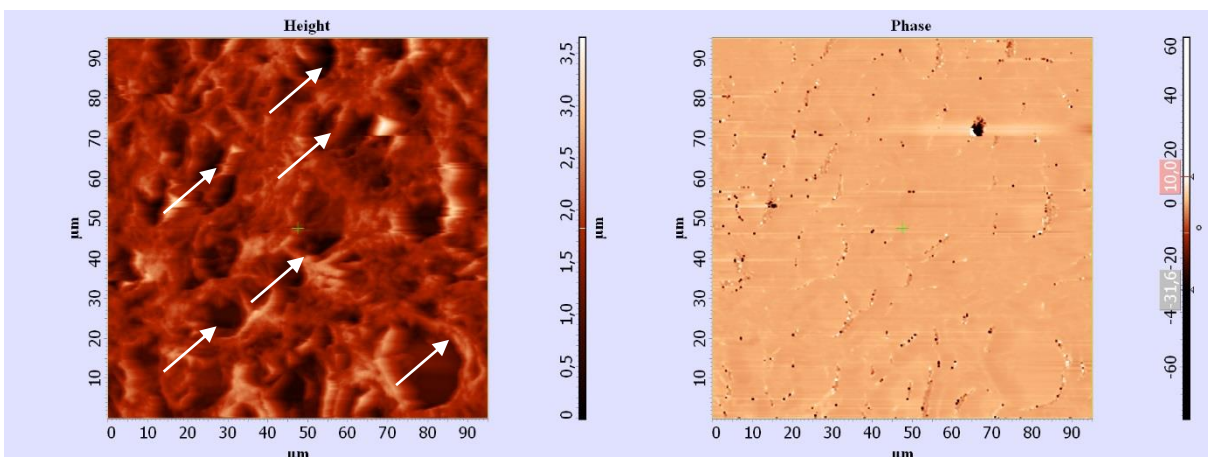


Fig. 14. AFM (left) and MFM (right) images of a sample of the common mushroom *Agaricus bisporus*: arrows indicate the hyphae.

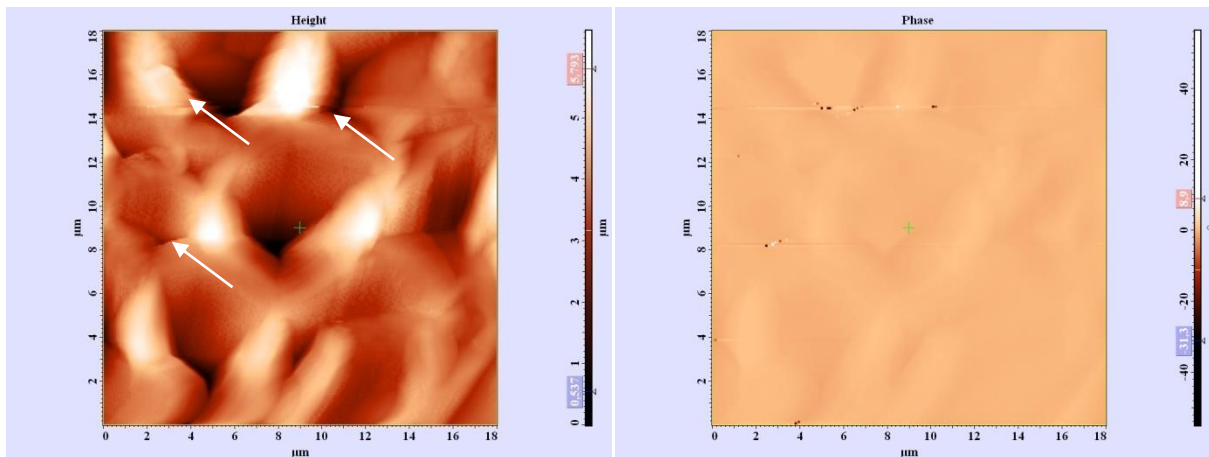


Fig. 15. AFM (left) and MFM (right) images of a sample of the shiitake mushroom *Lentinula edodes*: arrows indicate the hyphae.

Thus, studies of BMNs in samples of organs and tissues of animals, plants and fungi, conducted in this work showed that:

- BMN in the organs of multicellular organisms form chains;
- BMN in multicellular organisms are part of the transport system. Thus, BMNs in animals are located in the walls of capillaries (all examined organs and tissues except the ethmoid bone) or in the vicinity of the capillaries (the ethmoid bone). BMNs in plants are located in the wall of the conducting tissue, namely in the wall of sieve tubes of the phloem. BMNs in fungi are located in the wall of the conducting tissue, namely in the walls of the vascular hyphae¹³⁴⁻¹³⁶.

Conclusions

The chains of BMN are components of the cells that form the walls of the capillaries of animals and the walls of the conducting tissue of plants and fungi. At the same time, the functions of the capillaries of animals and the functions of the conducting tissue of the phloem of plants, as well as the vascular hyphae of fungi, are similar^{122,137,138}. In particular, capillaries (exchange vessels) exchange nutrients, gases, liquids, metabolites, signal substances (hormones), immune cells, etc. between the blood and body tissues^{137,139-141}. Conducting tissue of the phloem of plants serves to transfer organic substances, hormones, etc. through the body¹²²⁻¹²⁶. The same functions have vascular hyphae of fungi^{138,142-144}. The location of BMNs in various organs and tissues of animals, plants and fungi as part of systems with similar functions cannot be accidental, taking on account that the genetically programmed mechanism of biosynthesis of BMNs arose at the beginning of evolution^{42,43,145-147}. Such localization of BMNs argues in favour of the idea that BMNs chains are directly involved in metabolic processes^{25,42,43,148-150} and perform vital functions. In addition, bioinformatics analysis showed that BMNs in multicellular organisms, as well as in magnetotactic bacteria¹⁵¹⁻¹⁵⁴, form inside the cell and are associated with the cell membrane^{8,9,15,34,39}. This means that the chains of BMNs in multicellular organisms are part of a new type of organelles with the ferrimagnetic properties – the ferrimagnetic organelles of a specific purpose. Such ferrimagnetic organelles create scattering magnetic fields of the order of several fractions of T and gradients of magnetic field induction of the order of 10^5 - 10^6 T/m in their vicinity, which can significantly affect the mass transfer processes near the cell membrane of vesicles, granules^{41,42,150}, organelles, structural elements of the membrane and others.

In connection with the foregoing, it is clear that an extremely important task is to search for the general functions of BMNs in various organs and tissues of multicellular organisms. To solve this problem, it is necessary to identify the types and functions of cells containing BMNs in various organs of multicellular organisms.

Materials and Methods

Atomic force microscopy and magnetic force microscopy. Determination of the presence of BMNs and the study of their localization in the investigated samples was carried out using the «Solver PRO-M» scanning probe microscope by atomic force microscopy (AFM) and magnetic force microscopy (MFM).

The magnetic probe MFM_LM series with chip size 3.4x1.6x0.3mm, coated by CoCr was used. This probe was used both for AFM and MFM imaging. The non-contact AFM (NC-AFM) mode was applied. The MFM scanning was carried out at the constant distance from the sample surface after AFM scanning. The probe “lift” height was 100 nm. The cantilever was calibrated using the test samples. Calibration of the probe was carried out immediately before the measurements.

The biological material was prepared before AFM and MFM scanning. Fixation of biological material was carried out in a 10% formalin solution. The duration of fixation was 24 hours. After that, the biological material was washed in distilled water and conducted through ethanol with increasing concentration (from 50% to 100%). The next stage was the impregnation of the with liquid paraffin at a temperature of 55°C. After the solidification of paraffin at room temperature, a paraffin block was obtained. Slices from a paraffin block 5 µm thick were obtained using a microtome. After receiving the slices, they were placed on slides. The last stage was the release of slices from the mounting medium.

References

1. Blakemore, R. P. Magnetotactic bacteria. *Science* **190**, 377–379 (1975).
2. Frankel, R. B., Blakemore, R. P. & Wolfe, R. S. Magnetite in freshwater magnetotactic bacteria. *Science* **203**, 1355–1356 (1979).
3. Sakaguchi, T., Burgess, J. G. & Matsunaga, T. Magnetite formation by a sulphate-reducing bacterium. *Nature* **365**, 47–49 (1993).
4. Faivre, D. & Godec, T. U. From Bacteria to Mollusks: The Principles Underlying the Biomineralization of Iron Oxide Materials. *Angew. Chem. Int. Ed.* **54**, 4728–4747 (2015).
5. Hsu, Ch.-Y., Ko, F.-Y., Li, Ch.-W., Fann, K. & Lue, J.-T. Magnetoreception System in Honeybees (Apismellifera). *PLoS ONE*. **4**, e395 (2007)
6. Maher, B. A. Magnetite biomineralization in termites *Proc Biol Sci.* **265**, 733–737 (1998).
7. Cranfield, C. G. et al. Biogenic magnetite in the nematode *Caenorhabditiselegans*. *Proc. Biol. Sci.* **271**, 436–439 (2004).
8. Mann, S., Sparks, N. H. C., Walker, M. M. & Kirschvink, J. L. J. Ultrastructure, morphology and organization of biogenic magnetite from sockeye salmon. *Exp. Biol.* **140**, 35–49 (1988).
9. Walcott, C., Gould, J. L. & Kirschvink, J. L. Pigeons have magnets. *Science* **205**, 1027–1029 (1979).
10. Vainshtein, M., Suzina, N., Kudryashova, E., & Ariskina, E. New magnet-sensitive structures in bacterial and archaeal cells. *Biology of the Cell* **94**, 29–35 (2002).
11. Gajdardziska-josifovska, M., McClean, R.G., Schofield, M.A., Sommer, C.V. & Kean, W.F., *Eur. J. Mineral* **13**, 863-870 (2001).
12. de Barros, H.G., Esquivel, D.M., Danon, J. & de Oliveira, L. P. Magnetotactic algae. *An. Acad. Bras. Cienc.* **54**, 257–258 (1982).
13. Suzuki, Y. et al. Sclerite formation in the hydrothermal-vent “scaly-foot” gastropod—possible control of iron sulfide biomineralization by the animal. *Earth and Planetary Science Letters* **242**, 39–50 (2006).
14. de Oliveira, J.F. et al. Ant antennae: are they sites for magnetoreception? *J. R. Soc. Interface* **7**, 143–152 (2010).
15. Gould, J.L., Kirschvink, J.L. & Deffeyes, K.S. Bees have magnetic remanence. *Science* **202**, 1026-1028 (1978).
16. Acosta-Avalos, D. et al. Isolation of magnetic nanoparticles from *pachycondyla marginata* ants. *J. Exp. Biol.* **202**, 2687–2692 (1999).
17. Lohmann, K. J. Magnetic Remanence in the Western Atlantic Spiny Lobster, *Panulirus Argus*. *J. Exp. Biol.* **113**, 29-41(1984).
18. Brassart, J., Kirschvink, J.L., Phillips, J.B. & Borland, S.C. Ferromagnetic material in the eastern red-spotted newt *notophthalmus viridescens*. *Exp. Biol.* **202**, 3155-3160 (1999)
19. Kirschvink, J.L. Magnetite Biomineralization and Geomagnetic Sensitivity in Higher Animals: An Update and Recommendations for Future Study. *Bioelectromagnetics* (1989).
20. Diebel, C.E., Proksch, R., Greenk, C.R., Walker, P.N. & Walker, M.M. Magnetite denies a vertebrate Magnetoreceptor. *Nature* **406**, 299-302 (2000).
21. Eder, S.H.K. et al. Magnetic characterization of isolated candidate vertebrate magnetoreceptor cell. *Proc. Natl. Acad. Sci.* **109**, 12022–12027 (2012).

22. Moore, A., Freake, S. M. & Thomas, I. M.. Magnetic Particles in the Lateral Line of the Atlantic Salmon. *Phil. Trans. R. Soc. Lond. B* **329**, 11-15 (1990).
23. Moore, A.& Riley, W.D. Magnetic particles associated with the lateral line of the European eel *Anguilla Anguilla*. *Journal of Fish Biology* **74**, 1629–1634 (2009).
24. Gorobets, S., Gorobets, O., Golub, V. & Gromnadska M. Ferromagnetic resonance in the ethmoid bones of salmon and silver carp. *Journal of Physics: Conf. Series.* **903**, (2017).
25. Gorobets, S., Gorobets, O., Bulaievskya, M. &Sharau I. Magnetic force microscopy of the ethmoid bones of migratory and non-migratory fishes. *Acta Physica Polonica A.* **3**, 734-737 (2018).
26. Oguram, Katom, Arain, Sasadat&Sakakyi. Magnetic particles in chum salmon (*Oncorhynchus keta*): extraction and transmission electron microscopy. *Can. J. Zool.* **70**, 874 – 877 (1992).
27. Irwin, W. P. & Lohmann, K. J. Disruption of magnetic orientation in hatchling loggerhead sea turtles by pulsed magnetic fields. *J. Comp. Physiol. A* **191**, 475–480 (2005).
28. Falkenberg, G. Avian Magnetoreception: Elaborate Iron Mineral Containing Dendrites in the Upper Beak Seem to Be a Common Feature of Birds. *PLoS ONE* **5**, (2010)
29. Fleissner, G., Fleissner, G., Stahl, B. &Falkenberg, G. Iron-mineral-based magnetoreception in birds: the stimulus conducting system. *J. Orintholog.***148**, 643–648 (2003).
30. Edwards, H.H., Schnell, G.D., DuBois, R.L. & Hutchison, V.H. Natural and Induced Remanent Magnetism in Birds. *The Auk* **109**, 43-56 (1992).
31. Edelman, N.B. et al. No evidence for intracellular magnetite in putative vertebrate magnetoreceptors identified by magnetic screening. *Proc. Natl. Acad. Sci.* **112**, 262–267 (2015).
32. Holland, R. A. and etc. Bats Use Magnetite to Detect the Earth’s Magnetic Field. *PLoS ONE* **3**, 1676 (2008).
33. Zoeger, J., Dunn, J. R. & Fuller, M. Magnetic material in the head of the common Pacific dolphin. *Science*, 892–894 (1981).
34. Kirschvink, J.L., Kobayashi-Kirschvink, A. & Woodford, B.J. Magnetite biomineralization in the human brain. *Proc. Natl Acad. Sci. USA.* **89**, 7683–7687 (1992).
35. Quintana, C., Cowley, J. M. &Marhic, C. Electron nanodiffraction and high-resolution electron microscopy studies of the structure and composition of physiological and pathological ferritin. *J. Struct. Biol.* **147**, 166–178 (2004).
36. Collingwood, J. F. et al. Three-dimensional tomographic imaging and characterization of iron compounds within Alzheimer's plaque core material. *J. Alzheimer’s Dis.* **14**, 235–245 (2008).
37. Grassi-Schultheiss, P.P., Heller, F.& Dobson, J. Analysis of magnetic material in the human heart, spleen and liver. *BioMetals* **10**, 351–355 (1997).
38. Kirschvink, J.L. Ferromagnetic crystals (magnetite?) in human tissue. *J Exp Biol.* **92**, 333–335 (1981).
39. Schultheiss-Grassi, P.P. &Dobson, J. Magnetic analysis of human brain tissue. *Biometals* **12**, 67–72 (1999).
40. Posfai, M. &Dunin-Borkowski, R. E. Magnetic Nanocrystals in Organisms. *Elements* **5(4)**, 235–240 (2009).
41. Gorobets, Yu.I. & Gorobets, S.V. *Bulletin of Herson State Technical University* **3**, 276–281 (2000).
42. Gorobets, O.Yu., Gorobets, S.V. &Gorobets, Yu.I. Biogenic Magnetic Nanoparticles. Biomineralization in Prokaryotes and Eukaryotes. *Dekker Encyclopedia of Nanoscience and Nanotechnology, Third Edition*, 300–308 (2014).
43. Gorobets, S.V. &Gorobets, O.Yu. Functions of biogenic magnetic nanoparticles in organisms. *Functional Materials* **1**, 18-26 (2012).
44. Bauer, G.B.et al. Magnetoreception and Biomineralization of Cetaceans, *Magnetite Biomineralization and Magnetoreception in Organisms* **5**, 489-507 (1985)
45. Walker, M. M., Kirschvink, J. L. &Dizon, A. E. Magnetoreception and biomineralization of magnetite Fish. *Magnetite biomineralization and magnetoreception in organisms*, 417–437 (1985).
46. Walker, M. M., Kirschvink, J. L., Chang, S. B. R. &Dizon, A. E. A candidate magnetic sense organ in the yellowfin tuna, *Thunnusalbacares*. *Science* **224(4650)**, 751–753 (1984).

47. Walker, M. M., Quinn, T. P., Kirschvink, J. L. & Groot, C. Production of single-domain magnetite throughout life by sockeye salmon, *Oncorhynchus nerka*. *Journal of Experimental Biology* **140**(1), 51–63 (1988).
48. Holland, R.A., Thorup, K., Vonhof, M.J., Cochran, W.W. & Wikelski, M. Navigation: Bat orientation using Earth's magnetic field. *Nature* **444**, 702 (2006).
49. Gorobets, S.V., Gorobets, O.Yu., Medvediev, O.V., Golub, V.O. & Kuzminykh L.V. Biogenic magnetic nanoparticles in lung, heart and liver. *Funct. Mater.* **24**, 405-408 (2017).
50. Gorobets, S. V., Medvediev, O., Gorobets, O. Y., & Ivanchenko, A. Biogenic magnetic nanoparticles in human organs and tissues. *Progress in Biophysics and Molecular Biology* **135**, 49–57 (2018).
51. Walker, M. M., Quinn, T. P., Kirschvink, J. L. & Groot, C. Production of single-domain magnetite throughout life by Sockeye Salmon, *Oncorhynchus nerka*. *J. exp. Biol.* **140**, 51-63 (1998).
52. Gorobets, S.V., Gorobets, O.Yu. & Demyanenko, I.V. Ferritin and biomineralization of magnetic nanoparticles in microorganisms. *Research Bulletin of NTUU "KPI"* **3**, 34-41 (2013).
53. Gorobets, O.Yu., Gorobets, S.V. & Sorokina, L.V. Biomineralization and synthesis of biogenic magnetic nanoparticles and magnetosensitive inclusions in microorganisms and fungi. *Functional Materials*. **21**, 427-436 (2014).
54. Kobayashi, A., Yamamoto, N. & Kirschvink, J. Studies of Inorganic Crystals in Biological Tissue: Magnetite in Human Tumor. *Reprinted from J. Jap. Soc. Powd. Metallurgy* **44**, 94–102 (1997).
55. Brem, F., Hirt, A.M. & Winklhofer, M. Magnetic iron compounds in the human brain: a comparison of tumor and hippocampal tissue. *J. R. Soc. Interface* **3**, 833–841 (2006)
56. Baker, R. R., Mather, J. G. & Kennaugh, J. H. Magnetic bones in human sinuses. *Nature* **303**, 78–80 (1983).
57. Melling, M., Karimian-Teherani, D., Mostler, S., Behnam, M., Hochmeister, S. 3-D morphological characterization of the liver parenchyma by atomic force microscopy and by scanning electron microscopy. *Microsc Res Tech.* **64**(1), 1-9 (2004).
58. Braet, F., Taatjes, D. & Wisse, E. Probing the unseen structure and function of liver cells through atomic force microscopy. *Seminars in Cell and Developmental Biology*, 1-54 (2017)
59. Braet, F., de Zanger, R., Seynaeve, C., Baekeland, M., & Wisse, E. A comparative atomic force microscopy study on living skin fibroblasts and liver endothelial cells. *J Electron Microsc.* **50**, 283-290 (2001)
60. Zapotoczny, B., Szafranska, K., Kus, E., Chlopicki, S. & Szymonski, M. Quantification of fenestrations in liver sinusoidal endothelial cells by atomic force microscopy. *Micron* **101**, 48–53 (2017).
61. Zapotoczny, B. et al. Atomic force microscopy reveals the dynamic morphology of fenestrations in live liver sinusoidal endothelial cells. *Scientific reports* **7**(1), 7994 (2017).
62. Mattsson, G., Jansson, L., & Carlsson, P.-O.. Decreased Vascular Density in Mouse Pancreatic Islets After Transplantation. *Diabetes* **51**(5), 1362–1366 (2002).
63. MacPhee, P. J., Schmidt, E. E. & Groom, A. C. Intermittence of blood flow in liver sinusoids, studied by high-resolution in vivo microscopy. *American Journal of Physiology-Gastrointestinal and Liver Physiology* **269**(5), G692–G698 (1995).
64. Yoon, Y. J. et al. Three-dimensional imaging of hepatic sinusoids in mice using synchrotron radiation micro-computed tomography. *PloS one* **8**(7), e68600 (2013).
65. Benten, D. et al. Hepatic targeting of transplanted liver sinusoidal endothelial cells in intact mice. *Hepatology* **42**(1), 140–148 (2005).
66. Goh, S.K. et al. Perfusion-decellularized pancreas as a natural 3D scaffold for pancreatic tissue and whole organ engineering. *Biomaterials* **34**, 6760-6772 (2013).
67. Simionescu, M., Simionescu, N. & Palade, G. E. Morphometric data on the endothelium of blood capillaries. *The Journal of cell biology* **60**(1), 128–152 (1974).
68. Henderson, J.R. & Moss, M.C. A morphometric study of the endocrine and exocrine capillaries of the pancreas. *Q J Exp Physiol.* **Jul;70**(3), 347-56 (1985).
69. Clementi, F. & Palade, G.E. Intestinal capillaries. I. Permeability to peroxidase and ferritin. *J Cell Biol.* **41**, 33-58 (1969).

70. Clementi, F. & Palade, G.E. Intestinal capillaries. II. Structural effects of EDTA and histamine. *J Cell Biol.* **42**, 706-714 (1969).
71. Wiedeman, M. P., Tuma, R. F. & Magrovitz, H. N. An introduction to microcirculation. *Biophysics and Bioenergetics Series 2*, (1981).
72. Bohlen, HG. Tissue PO₂ in the intestinal muscle layer of rats during chronic diabetes. *Circ Res.* **52**, 677-682 (1983)
73. Townsley, M. I. Structure and composition of pulmonary arteries, capillaries, and veins. *Comprehensive Physiology* **2(1)**, 675–709 (2011).
74. Sicard, D., Fredenburgh, L. E. & Tschumperlin, D. J. Measured pulmonary arterial tissue stiffness is highly sensitive to AFM indenter dimensions. *Journal of the mechanical behavior of biomedical materials* **74**, 118-127 (2017).
75. Gruber, S., Spielauer, I., Böhme, S., Baron, D., Markstaller, K., Ullrich, R., & Klein, K. U. Real-time in-vivo imaging of pulmonary capillary perfusion using probe-based confocal laser scanning endomicroscopy in pigs. *European Journal of Anaesthesiology* **32(6)**, 392–399 (2015).
76. Winkler, G. C. & Cheville, N. F. Morphometry of postnatal development in the porcine lung. *The Anatomical Record* **211(4)**, 427–433 (1985).
77. Schiraldi, L. et al. Functional Capillary Density for in Vivo Estimation of Intestinal Perfusion using Real-Time Confocal Endomicroscopy. *Journal of Cytology & Histology* **6(4)**, 1 (2015).
78. Winkler, G. C. & Cheville, N. F. Postnatal colonization of porcine lung capillaries by intravascular macrophages: An ultrastructural, morphometric analysis. *Microvascular Research* **33(2)**, 224–232 (1987).
79. Peñuela, L., Villaggio, B., Raiteri, R., Fiocca, R., & Vellone, V. G. Kidney Ultrastructure by Atomic Force Microscopy Imaging Directly From Formalin Fixed-Paraffin Embedded Biopsy: Is This a Dream Come True? *International Journal of Surgical Pathology* **10**, 1–2 (2017).
80. Sun, D. et al. Experimental coronary artery stenosis accelerates kidney damage in renovascular hypertensive swine. *Kidney international* **87(4)**, 719–727 (2015).
81. Khairoun, M., van den Heuvel, M., van den Berg, B.M., Sorop, O., de Boer, R., van Ditzhuijzen, N.S., et al. Early Systemic Microvascular Damage in Pigs with Atherogenic Diabetes Mellitus Coincides with Renal Angiopoietin Dysbalance. *PLoS ONE* **10(4)**, e0121555 (2015).
82. Tiedemann, K. & Egerer, G. Vascularization and glomerular ultrastructure in the pig mesonephros. *Cell and tissue research* **238(1)**, 165–175 (1984).
83. Vodenicharov, A. & Simoens, P. Morphologic Peculiarities of the Renal Cortical Vasculature Connected with Blood Redistribution in the Kidney of the Domestic Pig. *Journal of Veterinary Medicine Series C* **27(4)**, 257–262 (1998).
84. Hubert, O. et al. Rat spleen in the course of Babesiamicroti invasion: histological and submicroscopic studies. *Acta Protozoologica* **56(2)**, 129-137 (2017).
85. Snook, T. Studies on the perifollicular region of the rat's spleen. *The Anatomical Record* **148.2**, 149–159. (1964).
86. Steiniger, B. S., Ulrich, C., Berthold, M., Guthe, M. & Lobachev, O. Capillary networks and follicular marginal zones in human spleens. Three-dimensional models based on immunostained serial sections. *PloS one* **13(2)**, e0191019 (2018).
87. Miyata, H., Abe, M., Takehana, K., & Satoh, M. Three-Dimensional Reconstruction of the Pig Sheathed Artery. *The Journal of Veterinary Medical Science* **55(5)**, 855–857 (1993).
88. Miyata, H., Abe, M., Takehana, K., Iwasa, K., & Hiraga, T. Electron Microscopic Studies on Reticular Fibers in the Pig Sheathed Artery and Splenic Cords. *The Journal of Veterinary Medical Science*, **55(5)**, 821–827 (1993).
89. Saxena, P. R. & Verdouw, P. D. Tissue blood flow and localization of arteriovenous anastomoses in pigs with microspheres of four different sizes. *Pflugers Archiv European Journal of Physiology* **403(2)**, 128–135 (1985).
90. Seki, A. & Abe, M. Scanning electron microscopic studies on the microvascular system of the spleen in the rat, cat, dog, pig, horse and cow. *The Japanese Journal of Veterinary Science* **47(2)**, 237–249 (1985).

91. Hautot, D., Pankhurst, Q.A., Khan, N. & Dobson, J.P. Preliminary evaluation of nanoscale biogenic magnetite in Alzheimer's disease brain tissue. *Proc. Roy. Soc. B.* **270**, S62–S64 (2003).
92. Chekchun, V.F., Gorobets, O.Yu., Gorobets, S.V. & Demianenko, I.V. Magnetically sensitive nanostructures of endogenous origin in Ehrlich's carcinoma cells. *Nanostructure materials science* **2**, 102–109 (2011).
93. Alekseeva, T. A., Gorobets, S. V., Gorobets, O. Yu., Demyanenko, I. V. & Lazarenko, O. M. Magnetic force microscopy of atherosclerotic plaques. *Medical Perspectives* **1**, 4–10 (2014).
94. Koralewski, M., Pochylski, M., Mitroova, Z., Timko, M., Kopcansky, P. & Melnikova, L. Magnetic birefringence of natural and synthetic ferritin. *Journal of Magnetism and Magnetic Materials* **323**, 2413–2417(2011).
95. Chuanlin, L., Yunan, H., Chenghua, G., Chengsheng, L. & Xiguang C. Properties of Biogenic Magnetite Nanoparticles in the Radula of Chiton Acanthochiton rubrolineatus Lischke. *Journal of Wuhan University of Technology-Mater. Sci. Ed.* **26**, 478-482 (2011).
96. Papaefthymiou, G.C. The Mössbauer and magnetic properties of ferritin cores. *Biochimica et Biophysica Acta (BBA)-General Subjects* **1800(8)**, 886–897 (2010).
97. Oshtrakh, M. I., Alenkina, I. V., Kuzmann, E., Klencsar, Z. & Siemionkin, V. A. Anomalous Mössbauer line broadening for nanosized hydrous ferric oxide cores in ferritin and its pharmaceutical analogue FerrumLek in the temperature range. *Journal of Nanoparticle Research* **16(4)**, 2363(2014).
98. Joos, A., Rümenapp, C., Wagner, F.E. & Gleich, B. Characterisation of iron oxide nanoparticles by Mössbauerspectroscopy at ambient temperature. *J MagnMagn Mater.* **399**, 123–129 (2016).
99. Jin, W.Y., Xu, G.Z., Scلابassi, J., Zhu, J.G, Bagic, A. & Sun, M.G. Detection of magnetic nanoparticles with magnetoencephalography. *J MagnMagn Mater.* **320**, 1472–1478 (2008).
100. Pan, Y. H. et al. 3D morphology of the human hepatic ferritin mineral core: New evidence for a subunit structure revealed by single particle analysis of HAADF-STEM images. *J. Struct. Biol.* **166(1)**, 22–31 (2009).
101. Quintana, C. et al. Initial studies with high resolution TEM and electron energy loss spectroscopy studies of ferritin cores extracted from brains of patients with progressive supranuclear palsy and Alzheimer disease. *Cellular and molecular biology* **46**, 807–820 (2000).
102. Gossuin, Y., D. Hautot, et al. (2005). Looking for biogenic magnetite in brain ferritin using NMR relaxometry. *NMR in Biomedicine* **18 (7)**, 469-472 (2005).
103. Passeri, D. et al. Magnetic force microscopy: quantitative issues in biomaterials. *Biomatter* **4**, e29507 (2014).
104. Daniels, S.L, Ngunjiri, J.N. &Garno, J.C. Investigation of the magnetic properties of ferritin by AFM imaging with magnetic sample modulation. *Anal. Bioanal. Chem.* **394**, 215-23 (2009).
105. Mikhaylova, A., Davidson, M., Toastmann, H., Channell, J.E.T., Guyodo, Y., Batich, C. & Dobson, J. Detection, identification and mapping of iron anomalies in brain tissue using X-ray absorption spectroscopy. *J. R. Soc. Interface* **2**, 33–37(2005).
106. Espinosa, A. et. al. On the discrimination between magnetite and maghemite by XANES measurements in fluorescence mode. *Meas. Sci. Technology* **23**, (2012).
107. Gálvez, N. et al. Comparative structural and chemical studies of ferritin cores with gradual removal of their iron contents. *J Am Chem Soc.* **130**, 8062-8068 (2008).
108. Melníková, L., Petrenko, V.I., Avdeev, M.V., Garamus, V.M., Almásy, L., Ivankov, O.I., Bulavin, L.A., Mitróová, Z.&Kopčanský, P. Effect of iron oxide loading on magnetoferritin structure in solution as revealed by SAXS and SANS. *Colloids Surf B Biointerfaces.* **123**, 82-8 (2014).
109. Pershant, P.S. Magneto-optical effects. *J Appl Phys.* **38**, 1482–1490 (1967)
110. Koralewski, M., Pochylski, M., Mitróová, Z., Melníková, L., Kovác, J., Timkoand, M.&Kopčanský, P. Magnetic Birefringence Study of the Magnetic Core Structure of Ferritin. *ActaPhysicaPolonica A.* **121**, 1237-1239(2012).
111. Koralewski, M., Kłos, J.W., Baranowski, M., Mitróová, Z., Kopčanský, P., Melníková, L., Okuda, M.&Schwarzacher, W. The Faraday effect of natural and artificial ferritins. *Nanotechnology.* **23(35)**, 355704 (2012).
112. Koralewski, M., Pochylski, M.&Gierszewski, J. Magnetic properties of ferritin and akaganeite nanoparticles in aqueous suspension. *J Nanopart Res.* **15**, 1902 (2013).

113. Dobosz, B., Krzyminiewski, R., Koralewski, M. & Hałupka-Bryl, M. Computer enhancement of ESR spectra of magnetite nanoparticles *J. Magn. Magn. Mater.* **407**, 114-121 (2016) .
114. Wajnberg, E., El-Jaick, L. J., Linhares, M. P. & Esquivel, D. M. Ferromagnetic resonance of horse spleen ferritin: core blocking and surface ordering temperatures. *Journal of magnetic resonance* **153(1)**, 69–74 (2001).
115. Hemmer, R., Hall, A., Spaulding, R., Rossow, B., Hester, M., Caroway, M., Haskamp, A., Wall, S., Bullen, H.A., Morris, C. & Haik, K. L. Analysis of biotinylated generation 4 poly(amidoamine) (PAMAM) dendrimer distribution in the rat brain and toxicity in a cellular model of the blood-brain barrier. *Molecules* **17;18(9)**, 11537-52 (2013).
116. Scheich, H., Honegger, H. W., Warrell, D. A. & Kennedy, G. Capillary dilatation in response to hypoxia in the brain of a gobiid fish. *Respiration Physiology* **15 (1)**, 87–95 (1972).
117. Miller, D. S., Graeff, C., Droulle, L., Fricker, S., & Fricker, G. Xenobiotic efflux pumps in isolated fish brain capillaries. *American Journal of Physiology-Regulatory, Integrative and Comparative Physiology* **282(1)**, R191–R198 (2002). doi:10.1152/ajpregu.00305.2001
118. Saladin, K. S., Sullivan, S. J. & Gan, C. A. Anatomy & physiology: the unity of form and function. *New York: McGraw Hill*, 1129 (2015).
119. Fehrenbach, M. & Herring S. Illustrated Anatomy of the Head and Neck. *Elsevier* **336** (2012).
120. Jacobs Human Anatomy. *Elsevier* **244**, 210 (2008).
121. Bharde, A., Rautray, D. & Sarkar I. Sastry Extracellular Biosynthesis of Magnetite using Fungi. *Small* **2**, 135-141 (2006)
122. Lalonde, S., Wipf, D. & Frommer, W.B. Transport mechanisms for organic forms of carbon and nitrogen between source and sink. *Annu Rev Plant Biol.* **55**, 341-72 (2004).
123. Buvat, R. Ontogeny, Cell Differentiation, and Structure of Vascular Plants. *Springer-Verlag Berlin Heidelberg XVII*, 581 (1989)
124. Raven, P. H., Evert, R. F. & Eichhorn, S.E. Biology of Plants, ed. 5th. *Worth Publishers* (1992).
125. Turgeon, R. & Wolf, S. Phloem transport: cellular pathways and molecular trafficking. *Annual review of plant biology* **60**, 207–221 (2009).
126. Lucas, W.J., Groover, A., Lichtenberger, R., Furuta, K., Yadav, S.R., Helariutta, Y., He, X.Q., Fukuda, H., Kang, J., Brady, S.M., Patrick, J.W., Sperry, J., Yoshida, A., López-Millán, A.F., Grusak, M.A. & Kachroo, P. The plant vascular system: evolution, development and functions. *J Integr Plant Biol.* **55(4)**, 294-388 (2013). doi: 10.1111/jipb.12041.
127. McCulloh, K.A., Sperry, J.S. & Adler, F.R. Water transport in plants obeys Murray's law. *Nature* **421**, 939-42 (2003).
128. Yeo, A. & Flowers, T. Plant solute transport. *Oxford UK: Blackwell Publishing*, 405 (2007).
129. Zimmermann, U. et al. What are the driving forces for water lifting in the xylem conduit? *Physiologia Plantarum* **114(3)**, 327–335 (2002).
130. Melvin, T. The cohesion-tension theory of sap ascent: current controversies. *Journal of Experimental Botany* **48 (10)**, 1753 (1997). doi:10.1093/jxb/48.10.1753.
131. Ding, X., Patel, M. & Chan, C.C. Molecular pathology of age-related macular degeneration. *Prog. Retin. Eye Res.* **28**, 1–18 (2009).
132. Mullendore, D.L., Windt, C.W., Van, As. H. & Knoblauch, M. Sieve tube geometry in relation to phloem flow. *Plant Cell* **22(3)**, 579-93 (2010). doi: 10.1105/tpc.109.070094.
133. Szymońska, J., Targosz-Korecka, M. & Krok, F. Characterization of starch nanoparticles. *Journal of Physics: Conference Series* **146(1)**, 012027 (2009).
134. Tian, Y., Zhao, Y., Huang, J., Zeng, H. & Zheng, B. Effects of different drying methods on the product quality and volatile compounds of whole shiitake mushrooms. *Food Chemistry* **197**, 714–722 (2016).
135. García-Segovia, P., Andrés-Bello, A. & Martínez-Monzó, J. Rehydration of air-dried Shiitake mushroom (*Lentinusedodes*) caps: Comparison of conventional and vacuum water immersion processes. *LWT - Food Science and Technology* **44**, 480-488 (2011).
136. Santana Nunes, J. et al. Evaluation of the infection process by *Lecanicillium fungicola* in *Agaricus bisporus* by scanning electron microscopy. *Revista Iberoamericana de micología* **34(1)**, 36-42 (2017).

137. Nagy, J.A., Benjamin, L., Zeng, H., Dvorak, A.M. & Dvorak, H.F. Vascular permeability, vascular hyperpermeability and angiogenesis. *Angiogenesis* **11**(2), 109-19 (2008).doi: 10.1007/s10456-008-9099-z.
138. Moore, D. R., Geoffrey, D. T. & Anthony, P. J. 21st Century Guidebook to Fungi. *Cambridge University Press*, 639 (2011).
139. Sukriti, S., Tauseef, M., Yazbeck, P. & Mehta, D. Mechanisms regulating endothelial permeability. *Pulmonary circulation* **4**(4), 535–551 (2014).
140. Bauer, H. & Pillana, A. EEG-based local brain activity feedback training—tomographic neurofeedback. *Frontiers in Human Neuroscience* **8**, (2014).
141. Guyton, A. C. Textbook of Medical Physiology. Philadelphia, Pennsylvania. *Elsevier Inc.* **11** (40):503 (2006).
142. Ramesh Maheshwari Fungi: Experimental Methods In Biology, *Second Edition 2nd Edition CRC Press*, 358 (2016).
143. Gooday, G. W. The dynamics of hyphal growth. *Mycological Research* **99**, 385–394 (1995).
144. Steinberg, G. Hyphal growth: a tale of motors, lipids, and the Spitzenkörper. *Eukaryotic cell* **6**(3), 351–360 (2007).
145. Chang, S. R. & Kirschvink, J.L. Magnetofossils, the magnetization of sediments, and the evolution of magnetite biomineralization *Annu. Rev. Earth Planet. Sci.* **17**, 169–195 (1989)
146. Chang, Shin-Bin, R., Stolz, J.F., Kirschvink, J.L. & Awramik, S.M. Biogenic magnetite in stromatolites. II. Occurrence in ancient sedimentary environments. *Precambrian Research* **43**, 305-315 (1989)
147. Ullrich, S., Kube, M., Schübbe, S., Reinhardt, R. & Schüler, D. A hypervariable 130-kilobase genomic region of *Magnetospirillum gryphiswaldense* comprises a magnetosome island which undergoes frequent rearrangements during stationary growth. *Journal of bacteriology* **187**(21), 7176–7184 (2005).
148. Gorobets, O.Yu., Gorobets, S.V. & Gorobets, Yu.I. Biomineralization of intracellular biogenic magnetic nanoparticles and their possible functions. *Research Bulletin of NTUU "KPI"*. **3**, 28–33 (2013).
149. Gorobets, O., Gorobets S. & Koralewski M. Physiological origin of biogenic magnetic nanoparticles in health and disease: from bacteria to humans. *Int J Nanomedicine* **12**, 4371–4395 (2017).
150. Mikeshyna, H., Darmenko, Y., Gorobets, O., Gorobets, S., Sharay, I. & Lazarenko, O. Influence of Biogenic Magnetic Nanoparticles on the Vesicular Transport. *Acta Physica Polonica A* **133** (3), 731-733 (2018).
151. Richter, M., Kube, M. & Bazylinski, D.A. Comparative Genome Analysis of Four Magnetotactic Bacteria Reveals a Complex Set of Group-Specific Genes Implicated in Magnetosome Biomineralization and Function. *Journal of Bacteriology* **189**(13), 4899–4910 (2007).
152. Fernanda, A., Mauricio, E.C. & Marisa, F.N. Common ancestry of iron oxide- and iron-sulfide-based biomineralization in magnetotactic bacteria. *The ISME* **5**, 1634–1640 (2011).
153. Grünberg, K., Müller, E., Otto, A., etc. Biochemical and Proteomic Analysis of the Magnetosome Membrane in *Magnetospirillum gryphiswaldense*. *Appl Env. Mic.* **70**, 1040–1050 (2004).
154. Arakaki, A., Nakazawa, H., Nemoto, M., Mori, T. & Matsunaga, T. Formation of magnetite by bacteria and its application. *J. R. Soc. Interface* **5**, 977–999 (2008).